Title

The effect of type 2 diabetes on CD36 expression and the uptake of oxLDL Diabetes affects CD36 and oxLDL uptake

Authors

Kanoke, Atsushi
Nishijima, Yasuo
Ljungberg, Magnus
et al.

Publication Date

2020-12-01

DOI

10.1016/j.expneurol.2020.113461

Peer reviewed

HHS Public Access

Author manuscript

Exp Neurol. Author manuscript; available in PMC 2021 December 01.

Published in final edited form as:

Exp Neurol. 2020 December ; 334: 113461. doi:10.1016/j.expneurol.2020.113461.

The effect of type 2 diabetes on CD36 expression and the uptake of oxLDL Diabetes affects CD36 and oxLDL uptake

Atsushi Kanoke[1,2,3,¶], **Yasuo Nishijima**[1,2,3,¶], **Magnus Ljungberg**[1,2,4,¶], **Shunsuke Omodaka**[1,2,3], **Shih Yen Yang**[1,2], **Suwai Wong**[1,2], **Gratianne Rabiller**[1,2], **Teiji Tominaga**[3], **Christine L Hsieh**[2,5], **Jialing Liu**[1,2,*]

[1]Department of Neurological Surgery, UCSF, San Francisco, CA 94158, USA

[2]Department of Neurological Surgery, SFVAMC, San Francisco, CA 94158, USA

[3]Department of Neurosurgery, Tohoku University Graduate School of Medicine, 1-1 Seiryo-machi, Aoba-ku, Sendai 980-8574, Japan

[4]Linköping University, SE-581 83 Linköping, Sweden

[5]Department of Medicine, UCSF

Abstract

We investigated whether type 2 diabetes mellitus (T2DM), a risk factor of stroke, affects the level of scavenger receptor CD36 and the uptake of its ligand, oxidized LDL (oxLDL); and whether pioglitazone, a drug that enhances CD36, promotes oxLDL uptake. Compared to normoglycemic db/+ mice, adult db/db mice showed a pronounced reduction in surface CD36 expression on myeloid cells from the blood, brain, and bone marrow as detected by flow cytometry, which correlated with elevated plasma soluble-CD36 as determined by ELISA. Increased CD36 expression was found in brain macrophages and microglia of both genotypes 7 days after ischemic stroke. In juvenile db/db mice, prior to obesity and hyperglycemia, only a mild reduction of

[*]**Corresponding author**: Department of Neurological Surgery (112C), University of California at San Francisco and Department of Veterans Affairs Medical Center, 1700 Owens Street, San Francisco, California 94158, USA., jialing.liu@ucsf.edu.

[¶]These authors contributed equally to this work.

Author Contribution Statement

Atsushi Kanoke performed the stroke induction, isolation of cells, FACS analysis, BMDM cell culture, overall data analysis, and contributed to manuscript writing

Yasuo Nishijima performed the stroke induction, isolation of cells, FACS analysis, overall data analysis, and contributed to manuscript writing

Magnus Ljungberg performed the BMDM cell culture, oxLDL uptake assay quantification and data analysis, and contributed to manuscript writing

Shunsuke Omodaka performed BMDM cell culture, and FACS analysis

Shih Yen Yang performed cell isolation and FACS analysis

Suwai Wong performed FACS analysis, statistical analysis and preparation of figures

Gratianne Rabiller performed oxLDL-uptake quantification and statistical analysis

Teiji Tominaga provided overall interpretation and clinical relevance of the study in type 2 diabetes

Christine L Hsieh performed FACS analysis and contributed to the overall knowledge of neuroinflammation

Jialing Liu provided the overall idea, design, analysis, logistics and writing of the manuscript.

Disclosure/Conflict of Interest: None

surface CD36 was found in blood neutrophils, while all other myeloid cells showed no difference relative to the db/+ strain. *In vivo*, oral pioglitazone treatment for four weeks increased CD36 levels on myeloid cells in db/db mice. *In vitro*, uptake of oxLDL by bone marrow derived macrophages (BMDMs) of db/db mice was reduced relative to db/+ mice in normal glucose medium. OxLDL uptake inversely correlated with glucose levels in the medium in db/+ BMDMs. Furthermore, pioglitazone restored oxLDL uptake by BMDMs from db/db mice cultured in high glucose. Our data suggest that T2DM is associated with reduced CD36 on adult myeloid cells, and pioglitazone enhances CD36 expression in db/db cells. T2DM or high glucose reduces oxLDL uptake while pioglitazone enhances oxLDL uptake. Our findings provide new insight into the mechanism by which pioglitazone may be beneficial in the treatment of insulin resistance.

Introduction

Atherosclerosis is the primary cause of heart disease and stroke in developed countries (Engstrom et al., 2003). Hyperglycemia exists in 30–40% of patients with acute ischemic stroke and is associated with a poor outcome after stroke (Fuentes et al., 2009; Martini & Kent, 2007; Parsons et al., 2002). Type 2 diabetes mellitus (T2DM) is a major risk factor in ischemic stroke (Emerging Risk Factors et al., 2010) and is independently associated with worse functional deficits after stroke (Megherbi et al., 2003). However, whether T2DM or hyperglycemia negatively impacts the uptake of oxLDL, which may promote atherosclerosis, is not well understood.

CD36, a transmembrane glycoprotein scavenger receptor for oxLDL, is expressed on various cells including monocytes, macrophages, platelets, adipocytes and microvascular endothelial cells (Febbraio, Hajjar, & Silverstein, 2001). The gene for the receptor is located on the chromosome 7 in humans. Apart from oxLDL, CD36 has the ability to bind other ligands, such as thrombospondin, A-beta amyloid, and components in microbes including malaria parasite P. Falciparum (Puente Navazo, Daviet, Ninio, & McGregor, 1996). According to the response-to-retention hypothesis, lipoprotein retention to the subendothelial compartment is a major contributor to atherosclerosis (Williams & Tabas, 1995). ApoB lipoproteins such as LDL are needed for the retention to the subendothelium, hence the sequestering capacity of CD36 comes into play. Consequently, low plasma levels of apoB or LDL are associated with decreased risk of heart diseases and stroke (Tabas, Williams, & Boren, 2007). Conversely, higher levels of oxLDL retained in the endothelium are directly chemoattractive to monocytes (Bisgaard et al., 2016; Cushing et al., 1990; Quinn, Parthasarathy, Fong, & Steinberg, 1987; Wang et al., 2013), triggering inflammation.

Owing to the essential role of CD36 in oxLDL uptake, CD36 deficiency in known to have a negative impact on human health. For example, two types of CD36 genetic deficiency have been reported in the African and Asian population. The type I phenotype is characterized by a deficiency of CD36 in monocytes, macrophages and platelets, whereas type II exhibits CD36 deficiency only in platelets (Hirano et al., 2003). Humans with CD36 deficiency also have higher plasma HbA1c levels as well as insulin resistance (Miyaoka et al., 2001). Moreover, compared to the general population, patients with CD36 deficiency showed a significantly increased rate of morbidity caused by cardiovascular diseases (Yuasa-Kawase

et al., 2012). Furthermore, markers of insulin resistance together with high levels of sCD36 are associated with an increased risk of T2DM (Handberg et al., 2010). Lastly, CD36-deficient patients with intracerebral hemorrhage (ICH) had a slower rate of hematoma adsorption and aggravated neurologic deficits (Fang et al., 2014), further attesting to the positive role of CD36 in human health.

The current study sought to determine the level of CD36 protein expression on myeloid cells in the blood, brain and bone marrow of diabetic db/db and normoglycemic control mice db/+, and to determine the effect of pioglitazone, a peroxisome proliferator-activated receptor gamma (PPARγ) agonist known to enhance CD36, on CD36 expression. For the functional assessment of CD36, we compared the uptake of oxLDL in bone marrow-derived macrophages (BMDMs) from two strains of mice under either normal or high glucose environment in vitro. Lastly, the study determined whether pioglitazone restored the uptake of oxLDL in BMDMs from both strains of mice in either glucose environment.

Material and methods

Mice and housing

db/db mice (B6.BKS(D)-Lepr*<db/db>*/J) carrying a point mutation in the leptin receptor gene were used as the model of obesity-induced T2DM. Heterozygous *db/+* mice (B6.BKS(D)-Lepr*<db/+>*/J) were used as euglycemic controls. Male db/db and db/+ mice (Jackson Laboratories, Sacramento, CA) were used in experiments involving experimental stroke to eliminate potential effects caused by sex hormones, while female mice as well as males were used in other experiments. Mice were housed 5 per cage on a 12h dark/light cycle with food and water access ad libitum. All animal experiments were conducted in accordance with the *Guide for Care and Use of Laboratory Animals*, and reported in compliance with *Animals in Research: Reporting In Vivo Experiments (ARRIVE) guidelines* (Kilkenny et al., 2011; Percie du Sert et al., 2019), and were approved by the San Francisco Veterans Affairs Medical Center Institutional Animal Care and Use Committee. Mice were coded at the beginning of the experiment. The identity of each mouse subject was blinded to investigators who conducted the experiments and data analysis.

Ischemic Stroke

Ischemic stroke was induced by distal middle cerebral artery occlusion (dMCAO) as previously described (Akamatsu et al., 2015). An incision was made on the scalp to expose the calvaria over the bilateral cerebral hemispheres. The left common carotid artery (CCA) was isolated and dissected out, with a nylon suture placed across the CCA from the bottom for future ligation. Along the sagittal suture, a straight skin incision was made, and the scalp was drawn back. After creating a 1.5 mm diameter burr hole 1.2 mm rostral to the anterior junction of the zygoma and temporalis bone with a dental drill, the dura was exposed with a fine needle. Then, the main trunk of the left MCA was permanently occluded with electric cauterizer. followed by transient ligation of the ipsilateral CCA for 60 minutes. Sham animals did not receive either MCA or CCA occlusion.

Peripheral Blood Mononuclear Cell isolation

Blood was collected by cardiac puncture with anti-coagulant ACD (Catalog No. sc-214744, Santa Cruz Biotechnology, Dallas, TX) and mixed with an equal volume of balanced salt solution (0.1 g/L anhydrous D-glucose, 0.00074 g/L $CaCl_2 \cdot 2H_2O$, 0.01992 g/L $MgCl_2 \cdot 6H_2O$, 0.04026 g/L KCl, 1.7565 g/L TRIS, 7.371 g/L NaCl). Mononuclear cells were collected from the interface between 2 layers following centrifugation at 500g for 30 min at 4°C in Ficoll-Paque gradient (Catalog No. 17-5446-02, GE Healthcare Life Sciences, Chicago, IL).

Brain Mononuclear Cell isolation

Three days post-surgery, ipsilateral forebrain hemispheres were harvested after cardiac perfusion with heparinized GKN buffer (8 g/L NaCl, 0.4 g/L KCl, 1.41 g/L Na_2HPO_4, 0.6 g/L NaH_2PO_4, 2 g/L D(+) glucose, pH 7.4). The tissues were digested in NOSE buffer (4.0 g/L $MgCl_2$, 2.55 g/L $CaCl_2$, 3.73 g/L KCl, 8.95 g/L NaCl, pH 6–7) supplemented with 200 U/ml DNase I (Catalog No. D5025-150KU, Sigma-Aldrich, St. Louis, MO) and 0.2 mg/ml collagenase type I (Catalog No. L5004196, Worthington Biochemical, Lakewood, NJ) at 37°C for 30 min. Thoroughly washed cells were subjected to an isotonic Percoll gradient (90% Percoll, Catalog No. 17-0891-01, GE Healthcare Life Sciences, Chicago, IL) by suspending cells in 4 mL of 1.03g/mL Percoll in GKN buffer/0.2%BSA and overlaying cell suspension on 4 mL of 1.095 g/mL Percoll in PBS/0.2%BSA. After centrifugation at 900xg for 20 min at RT, the cells were collected from the interface, washed, and processed further for FACS staining and analysis.

Bone marrow isolation

Isoflurane sedation followed by cervical dislocation were used to sacrifice the mice. The tibia and femur were removed, the bone ends were carefully snipped off, and the bone marrow was flushed out with Mg^{2+}/Ca^{2+}-rich PBS. After centrifugation, the bone marrow pellet was resuspended and treated with 5 mL of 1X red blood cell (RBC) lysis buffer (Catalog No. 00-4333-57, eBioscience, San Diego, CA) for 5 min and thoroughly washed with PBS. After washing, the mononuclear cells were collected and processed.

Bone marrow-derived macrophages (BMDM)

After isolating the bone marrow, the cells were plated into 3 non-TC coated petri dishes 10 cm in diameter per femur and tibia. The cells were cultured in MEM-alpha (Catalog No. 012571-063, Thermo Fisher Scientific, Waltham, MA) supplemented with 10% FBS, penicillin-streptomycin, glutamine, and 15% CMG-conditioned medium containing M-CSF for 7 days in a 37°C, 5% CO_2 incubator. On day 8, the confluent cells were harvested following incubation in enzyme-free cell dissociation buffer (Catalog No. 13151-014, Life Technologies), and stored frozen at −80°C in Recovery Cell Culture Freezing Medium (Catalog No. 12648010, Thermo Fisher Scientific) for future use. Frozen cells were thawed and cultured overnight in a 37°C, 5% CO_2 incubator in either medium containing 5 mM glucose (normal glucose environment) or 25 mM glucose (high glucose environment) to mimic hyperglycemia.

Flow Cytometry

Mononuclear cells were suspended in 100 μL FACS buffer and blocked with 1μL anti-mouse CD16/CD32 (clone 93, Catalog No. 14-0161-85, eBioscience) for 20 min. The cells were immunostained for 30 min in the dark with 1μL of each of the following antibodies against: CD11b (clone M1/70, PerCP 5.5, Catalog No. 45-0112-82, eBioscience), CD45 (clone 30-F11, FITC, Catalog No. 11-0451-81, eBioscience), Ly6G Gr-1 (clone 1A8-Ly6G, PE-eFluor 610, Catalog No. AB_2574679, eBioscience), CD36 (clone CRF D-2712, PE, Catalog No. 562702 BD Pharmingen; clone 72-1,PE, Catalog No. 12-0361-82, eBioscience), IgG Isotype control (clone M18-254, PE, Catalog No. 562141, BD Pharmingen; clone eBR2a, PE, Catalog No. 12-4321-82, eBioscience), and fixable viability dye (eFluor 506, Catalog No. 65-0866-14, eBioscience). 50 μL Absolute counting beads (Catalog No. C36950, Life Technologies, Carlsbad, CA) were used for cell counting. After washing, the cells were resuspended in 100 μL of FACS buffer and 100 μL 2% PFA. Data were acquired using a BD FACS ARIAIII and were analyzed using FlowJo v10 software (FlowJo). BMDM cell death rate was calculated as (100%- %viability).

ELISA

The concentration of soluble CD36 (sCD36) in platelet poor plasma was measured by Mouse CD36 ELISA kit (Catalog No. ELM-CD36, RayBiotec, Peachtree Corners, GA) according to manufacturer's instructions. The detection range was between 30 pg/mL and 20,000 pg/mL.

oxLDL uptake assay

db/+ and db/db BMDM were plated in 96-well plates at 1–3 × 10^4cells/well and incubated overnight in 37°C, 5% CO_2. The following day, half of the plates were incubated at 37°Cwith DiI-labeled oxLDL (Catalog No. L34357, 10 μg/ml) in either normal (5 mM) or high (25 mM) concentration of glucose for 2 hrs. Cells were harvested, fixed with 2% PFA for 15 min on the shaker, and washed thoroughly with 0.1 M PB. They were then counterstained with DAPI (0.1 ug/mL) for 15 mins on the shaker at RT. After thoroughly washing the cells with 0.1M PB, they were stored in PB with 0.2% sodium azide at 4 °C until further analysis. The remaining other half of cells were incubated with antibodies to FITC-anti-mouse CD45 (clone 30-F11, Catalog No. 11-0451-81, eBioscience, 1:50 dilution) and PE-anti-mouse CD36 (clone CRF D-2712, Catalog No. 562702 and 72-1, Catalog No. 12-0361-82) for 30 minutes followed by washing in PBS and fixing in 4% PFA.

DiI signals were examined using high speed widefield/confocal microscopy (Nikon Ti Microscope, Andor Borealis CSU-W1 spinning disk confocal, 40x/0.95 Plan APO lens). Five random images/well were captured for quantification and analysis. Images were coded and the identity of the cells and treatment were blinded to the examiner who performed cell counting based on oxLDL uptake intensity. Briefly, mean fluorescence intensity values were determined from the binary image of the RGB microscope images in Fiji. Cells were counted using "Analyze particles" under the Fiji tool kit with a minimum threshold of 170 and size between 15–300 pixels. Mean intensity values between 170 to 230 were categorized as low uptake cells, 230–300 as medium uptake cells and 300–400 as high uptake cells. False positives were excluded for cells with a maximum intensity over 1000.

Pioglitazone Treatment

Twenty weeks old db/+ and db/db mice were randomly divided into two groups and treated with a regular diet (vehicle) or a pioglitazone (Catalog No. H60507MD, Alfar Aesar, Haverhill, MA)-supplemented diet (120 ppm pioglitazone chow diet, Envigo, Huntingdon, UK) for 4 weeks. At the end of 4 weeks, mice were subjected to an oral glucose tolerance test to determine treatment effect on insulin sensitivity. Mice were sacrificed the following day, and brains were harvested for FACS analysis. Additionally, 10 μMand 20 μM pioglitazone/0.01% DMSO were used to compare the uptake of DiI-labeled oxLDL in BMDM cultured in the presence of normal (5 mM) or high (25 mM) glucose for 24 hr in medium. 0.01% DMSO was used as the vehicle control.

Statistical Analysis

Data were expressed as Mean ± SD. The Kolmogorov-Smirnov normality test was used to determine whether data were normally distributed. Log transformation was used to bring back normality of data in Figure 6B. Data were analyzed by one-way ANOVA (Figures 3, 4, 8A-D), or two-way ANOVA for strain and temporal effects (Figure 2), strain and pioglitazone effects (Figure 5A, C&D, 8C) or for strain and glucose effects (Figure 6B, 6F-G, 7, 8B); followed by Tukey's multiple comparisons test using Prism 8 (GraphPad Software Inc., San Diego, CA). P values less than 0.05 were considered significant.

Results

Reduced expression of CD36 found in myeloid cells in the blood and brain of db/db compared to db/+mice

The mean intensity of CD36 expression detected by flow cytometry was reduced in several populations of myeloid cells in the adult db/db mice compared to db/+ mice according to the gating schemes designed for brain or blood mononuclear cells, respectively (representative cell gates are shown in Figure 1). Neutrophils, microglia and macrophages/monocytes are defined as cells expressing $CD45^{hi}/Ly6G^{hi}$, $CD45^{int}/Ly6G^{low}/CD11b^{hi}$ and $CD45^{hi}/Ly6G^{low}/CD11b^{hi}$, respectively. Experimental stroke enhanced surface expression of CD36 in brain macrophages and microglia 7 days after stroke in both db/+ and db/db mice, and also 3 days after stroke for db/+ mice (Figure 2A), while it did not significantly alter CD36 level in the blood cells of either genotype (Figure 2B). An overall reduction of CD36 expression was found in the db/db mice compared to db/+ mice regardless of time frame for brain macrophages (two-way ANOVA, genotype effect, $P<0.0001$), blood neutrophils ($P<0.0005$) and monocytes ($P<0.0001$). Specifically, monocytes and neutrophils in db/db blood expressed significantly reduced levels of CD36 compared to those in db/+ mice after stroke and at baseline, respectively. However, the level of soluble CD36 was significantly increased in the plasma of adult db/db mice compared to db/+ mice as detected by ELISA (db/db: 21,234±13,116 pg/ml; $p<0.0001$, db/+: 4,120±1,215 pg/ml; two-tailed unpaired t test; n=14/genotype).

db/db mice display reduced expression of CD36 in freshly isolated monocytes and T cells from bone marrow

We then determined CD36 expression on cells isolated from a third tissue, the bone marrow. Monocytes, granulocytes, T-like and B-like cells were defined as cells expressing CD45+/CD11b^{+}/Ly6G^{-}, CD45+/CD11b^{+}/Ly6G^{+}, CD45+/CD3^{hi}/CD45R^{low}, CD45+/CD3^{low}/CD45R^{hi}, respectively. The mean intensity of CD36 expression was also found to be significantly reduced in freshly isolated bone marrow monocytes and T-like cells in the db/db mice compared to db/+ mice (Figure 3). This suggests that the myeloid cells from diabetic mice displayed reduced surface expression of CD36 compared to control mice.

Brain macrophages and blood monocytes of juvenile db/db mice have similar level of CD36 compared to age-matched db/+ mice

We compared the expression of CD36 by FACS in myeloid cells isolated from brain or blood of db/+ and db/db mice at 3 weeks old, an age prior to the onset of obesity. We found that almost all myeloid cells except for blood neutrophils of juvenile db/db mice expressed comparable levels of CD36 compared to age-matched db/+ cells (Figure 4). There was a 20% reduction of CD36 expression in blood neutrophils of young db/db compared to young db/+ mice, which was a smaller reduction relative to that in the adult mice.

Pioglitazone enhances insulin sensitivity and increases CD36 expression on brain macrophages.

Adult db/+ and db/db mice (5 months of age) were treated with vehicle (regular diet) or the pioglitazone-supplemented diet (pioglitazone: 120 ppm, Envigo) for 4 weeks. At the end of treatment, they were subjected to an oral glucose tolerance test and their brains were collected for FACS analysis the following day. Two-way repeated measure ANOVA found significant effects of genotype ($p<0.0001$) and pioglitazone treatment ($p<0.0001$) on blood glucose levels. Although the glucose level was significantly higher in vehicle treated db/db mice compared to db/+ mice, pioglitazone effectively reduced blood glucose level from 15 to 90 minutes after oral glucose intake in the db/db mice (Figure 5A). Myeloid cells from the brain and blood of adult db/db mice had significantly lower expression of CD36 (expressed as mean fluorescence intensity, MFI) compared to that of db/+, while pioglitazone restored CD36 surface expression of db/db cells to similar levels as in the db/+ cells (Figure 5B-D).

Uptake of oxLDL is reduced in bone marrow macrophages of diabetic mice relative to control mice or in the presence of hyperglycemia

We next determined the functional consequences of reduced surface expression of CD36. Because CD36 binds oxLDL, we compared the uptake of DiI-labeled oxLDL in cultured BMDM of db/+ and db/db mice. To mimic the effect of hyperglycemia, we also compared the BMDM DiI-oxLDL uptake in the presence of normal (5 mM) or high (25 mM) concentration of glucose (Figure 6). We found that both glucose and genotype affect oxLDL medium uptake (genotype effect: $F_{1,28} = 11.95$, $p<0.005$; glucose effect: $F_{1,28} = 12.3$, $p<0.005$; interaction: $F_{1,28} = 5.95$, $p<0.05$) and low uptake (genotype effect: $F_{1,28} = 8.95$, $p<0.01$; glucose effect: $F_{1,28} = 8.74$, $p<0.01$; interaction: $F_{1,28} = 5.01$, $p<0.05$). Specifically, db/db BMDM displayed a reduced uptake of DiI-oxLDL compared to db/+ BMDM in

the normal glucose medium, and that db/+ BMDM cultured in high glucose medium reduced uptake of oxLDL compared to those cultured in normal glucose medium, consistent with clinical observation that T2DM and hyperglycemia can independently impact oxLDL clearance (Figure 6).

The total numbers of phagocytotic macrophages with engulfed oxLDL tended to be less in groups cultured in the high glucose environment (glucose effect: P= 0.06; genotype effect: P= 0.08) (Figure 6F). The observed difference in oxLDL uptake was not entirely correlated with cell viability, since two-way ANOVA revealed a global glucose ($P<0.05$) but no genotype effect on cell death (Figure 6G).

Pioglitazone restores oxLDL uptake in BMDM derived from diabetic mice

We then determined whether pioglitazone, the drug that increased CD36 expression in the myeloid cells in the blood and brain in the current study, can also rescue or reverse diabetes- or hyperglycemia-reduced uptake of oxLDL in BMDMs. We compared uptake of Dil-labeled oxLDL in BMDM cultured in normal (5mM) or high (25mM) glucose and treated with pioglitazone for 24 hours in media. Two concentrations were chosen for the pioglitazone treatment, a concentration of 10uM and 20uM, compared to a vehicle control with DMSO (10uM). We found that pioglitazone treatment enhanced oxLDL uptake only in the db/db BMDM cultured in hyperglycemic condition (Figure 7). Although there was trending effect of pioglitazone on improving oxLDL uptake in db/+ cells cultured in hyperglycemic medium, or db/db cells cultured in normoglycemic medium, the treatment effect did not reach statistical significance owing to large variance among these groups.

To test whether the observed difference in oxLDL uptake between genotypes, glucose concentrations or pioglitazone treatment was attributed to the difference in CD36 expression, CD36 MFI was quantified by FACS in BMDMs derived from both genotypes and cultured in either normal or high concentration of glucose containing medium. Surprisingly, db/db BMDM cells expressed very high but similar levels of CD36 compared to those of db/+ BMDMs (Figure 8A&B), suggesting that bone marrow cells were altered in *in vitro* culture in the presence of MCSF. There was also no significant difference in the level of CD36 expression between normal and high concentration of glucose containing media (Figure 8B). Consistent with the FACS data, immunofluorescence staining of BMDM cells cultured in the high glucose containing medium also failed to show genotype difference (Figure 8C).

Discussion

While the critical role of CD36 in eliciting inflammation during the formation of foam cells and atherosclerosis has been well established (Lusis, 2000; Nagy, Tontonoz, Alvarez, Chen, & Evans, 1998; Puente Navazo et al., 1996; Tontonoz, Nagy, Alvarez, Thomazy, & Evans, 1998), it still remains unclear whether CD36 expression is altered in type 2 diabetes and how it affects the uptake of oxLDL. Using a mouse model of type 2 diabetes, we found that the surface expression of CD36 was reduced on macrophages in the brain, as well as neutrophils and monocytes in the blood of the diabetic db/db mice compared to that of the normoglycemic control db/+ mice. In addition, ischemic stroke significantly increased the level of CD36 in brain macrophages and microglia of both genotype of mice 7 days

after stroke, consistent with the finding of a recent report (Woo, Yang, Beltran, & Cho, 2016). Furthermore, the expression of CD36 in bone marrow monocytes and T cells of the db/db mice was significantly reduced compared to those of the db/+ mice, although there was no significant genotype difference in CD36 level once these cells were cultured in MCSF. Diabetes-associated reduction of CD36 in murine myeloid cells coincided with an elevated level of soluble CD36 in the plasma, a feature well-reported in patients with T2DM (Handberg et al., 2010). Interestingly, the expression of CD36 in most myeloid subsets was comparable between two genotypes of 3-week old juvenile mice, an age prior to the onset of obesity and hyperglycemia in db/db mice. Further, the db/db phenotype or high glucose environment interfered with the uptake of oxLDL in BMDMs in vitro. We also found that pioglitazone restored CD36 expression in brain and blood myeloid cells of db/db mice and it had a borderline effect on improving oxLDL uptake of db/db BMDM cells cultured in high glucose medium.

The role of CD36 in the atherosclerotic process, inflammation, phagocytosis and the resolution of inflammation is complex and can be paradoxical. Upon receptor binding, CD36 activates inflammatory mediators such as Interleukin-1-beta (IL-1β) and tumor necrosis factor-alpha (TNF-α) (Yamashita et al., 2007) through the NLRP3 inflammasome, and upregulated secretion and assembly of the IL-1 family, as well as the Nod-like receptor (Rathinam, Vanaja, & Fitzgerald, 2012; Sheedy et al., 2013). Consistent with the deleterious role of CD36 in inflammation, mice null for CD36 were deficient in oxLDL or fatty acid uptake (CT Coburn et al., JBC 2000 275:32523–29) and therefore had fewer atherosclerotic lesions and plaque formations (Febbraio et al., 2000), pointing to a beneficial effect of CD36 deficiency in mice. The same group of investigators also found that CD36 KO adult mice had reduced inflammation and brain injury after transient MCAO (Cho et al., 2005; Kim, Tolhurst, Szeto, & Cho, 2015). However, others reported a larger injury in the same CD36 KO mouse line compared to WT mice after an acute neonatal stroke (Woo et al., 2012). This opposing finding might be attributed to the diminished removal of apoptotic neuronal debris in the absence of CD36 (Woo et al., 2012), suggesting a crucial role of CD36 in the resolution of inflammation. This was further supported by another study that cell-surface CD36 in monocytes/ macrophages contributed to phagocytosis during the resolution phase of ischemic stroke in mice (Woo et al., 2016). Furthermore, CD36 KO mice were reported to have decreased hematoma absorption with worse neurologic impairment, and increased TNF-α and IL-1β expression levels. Moreover, the phagocytic capacity of CD36 KO microglia for RBCs was concurrently decreased, while Toll-like-receptor 4 inhibitor TAK-242 upregulated CD36 expression in microglia and promoted hematoma absorption (Fang et al., 2014).

Findings regarding CD36 level in various pathological conditions have also been controversial. Some studies reported that hyperglycemia and insulin resistance upregulated CD36 expression on the surface of monocytes (Griffin et al., 2001; Liang et al., 2004; Sampson, Davies, Braschi, Ivory, & Hughes, 2003), while others found that humans with CD36 deficiency had higher HbA1c plasma and insulin resistance (Miyaoka et al., 2001). Additional evidence linking CD36 and metabolism came from the significantly increased rate of morbidity caused by cardiovascular diseases among CD36-deficient patients (Yuasa-Kawase et al., 2012) possibly due to reduced capacity in fatty acid uptake, as it was also

observed in CD36 KO mice (Coburn et al., 2000) and in SHR rats in which the deficiency of CD36 in the latter was genetically linked to the phenotype of hypertriglyceridemia and hyperinsulinemia (Hajri et al., 2001). Second, CD36 also plays a critical role in the response to inflammation. CD36-deficient patients had aggravated neurologic deficits after intracerebral hemorrhage owing to a slower hematoma adsorption rate (Fang et al., 2014). Interestingly, CD36 mutation occurs at an exceptionally high frequency within the population of malaria-endemic regions, although any selective advantage of CD36 deficiency in reducing parasite sequestration has not been confirmed in the context of reduced innate immune response (Aitman et al., 2000; Pain et al., 2001). Furthermore, markers of insulin resistance together with high levels of sCD36 are associated with an increased risk of T2DM (Handberg et al., 2010). In keeping with these human data, we found that insulin-resistant db/db mice exhibited a reduced level of surface expression of CD36 on myeloid cells in three tissue compartments and an increased soluble level of CD36 in the plasma compared to their db/+ littermates. Most importantly, the reduction of myeloid CD36 was not seen in juvenile db/db mice except for a mild decrease in blood neutrophils, suggesting that the reduction of CD36 appears to coincide with pathological changes associated with obesity and hyperglycemia. However, in contrast to our findings, a recent paper reports that salvianolic acid B, a CD36 antagonist that blocks macrophage uptake of oxLDL, reduces visceral fat accumulation and improves insulin resistance in obese $BDNF^{M/M}$ mice that have increased CD36 expression (Yang, Park, & Cho, 2018). The discrepancy in findings may be due to the different genetic models for experimental obesity or insulin resistance studied.

Pioglitazone, a PPARγ agonist, has shown efficacy in reducing secondary stroke risk in patients with insulin resistance in recent IRIS trials (Yaghi et al., 2018). Consistent with the reported effect of pioglitazone on increasing CD36 expression (Eto, Sumi, Fujimura, Yoshikawa, & Sakoda, 2008; Liu et al., 2014), our FACS data demonstrated a restoration of CD36 expression in brain macrophages and blood monocytes of db/db mice after the treatment, coincident with improved performance on the glucose tolerance test. Pioglitazone also increased CD36 expression in BMDM cells, although there was no genotype difference. In contrast to previous findings, TAK-242 did not affect CD36 expression in either blood or brain myeloid cells of db/db adult mice in our experiment (data not shown).

Because polymorphisms in the CD36 gene have been linked to abnormal lipid metabolism and susceptibility to the metabolic syndrome, one likely outcome for a reduced level of CD36 in the myeloid cells would be a decrease in oxLDL uptake, which in turn diminishes the capacity of lipid clearance and increases overall risk of atherosclerosis and vascular diseases. We found that when cultured in a normal concentration of glucose, BMDMs from db/db mice displayed reduced oxLDL uptake compared to that in db/+ mice, while in a high glucose environment, oxLDL uptake was decreased in both genotypes, suggesting that either the diabetic phenotype or high glucose environment interferes with oxLDL uptake in the BMDMs. When tested in vitro, we found that pioglitazone at 20 μM had a borderline effect ($P = 0.065$) on improving oxLDL uptake only in the db/db BMDMs cultured in high glucose medium.

Emerging evidence suggests that CD36 is involved in the phagocytosis of apoptotic cells, known as efferocytosis (Greenlee-Wacker, 2016). The cleavage of CD36 by ADAM17 family of proteases (Driscoll, Vaisar, Tang, Wilson, & Raines, 2013; Jiang et al., 2017) impedes efferocytosis and interferes with the resolution of inflammation (Driscoll et al., 2013), while knockdown of Rab11a reduced ADAM17 and increased the surface level of CD36 in macrophages (Jiang et al., 2017). Pioglitazone also normalizes the defective efferocytosis in monocytes from patients with chronic granulomatous disease (Fernandez-Boyanapalli et al., 2015), supporting another functional role of CD36 in mediating recovery. We have not determined whether reduced CD36 is due to proteolytic cleavage, let alone whether it is ADAM17-dependent. Further investigation is warranted to determine the link between the increased soluble CD36 and the reduction of CD36 on the cell surface owing to proteolytic cleavage and to identify proteases involved should it occur, as well as the mechanism by which T2DM activates the process. Nonetheless, the increased sCD36 in the plasma of db/db mice is akin to that of T2DM patients, and the reduced CD36 expression in the myeloid cells of db/db mice is in line with CD36-deficient humans that exhibit insulin resistance (Handberg et al., 2010; Miyaoka et al., 2001; Yuasa-Kawase et al., 2012).

One major limitation of our study is the lack of a causal link between the level of CD36 and oxLDL uptake from the available data. Although reduced CD36 expression was found on freshly isolated myeloid cells of adult db/db mice from blood, brain and BM compared to db/+ mice, there was no genotype difference in cultured BMDMs. A direct explanation for this discrepancy is that the former ex vivo cells from db/db mice have been exposed to the inflammatory milieu caused by obesity and T2DM, which may have led to the reduction of CD36. However, BMDM cells have been differentiated in MCSF-containing medium for one week and their expression of CD36 was much higher compared to ex vivo myeloid cells from either genotype. Another technical limitation we encountered is the inability to perform oxLDL uptake in freshly isolated myeloid cells owing to the lack of adherence of cells to plates needed for quantification, excluding the possibility to establish a direct correlation between the level of CD36 and oxLDL uptake. A third limitation is that we did not address whether the reduced MFI in CD36 staining in the db/db myeloid cells was due to a reduced amount of CD36 protein on cell surface, or reduced binding affinity to antibody. Appropriate antibody reagents recognizing various domains or epitopes of CD36 are needed to determine if there are different forms of CD36 inside the cells and to characterize the increased soluble fraction in the plasma of db/db.

In conclusion, we found that CD36 levels were reduced in the myeloid cells in multiple tissue compartments of the adult but not juvenile diabetic db/db mice compared to age-matched normoglycemic littermates db/+ mice. The adult db/db mice also have increased levels of soluble CD36 in the plasma, similar to patients with T2DM. Both diabetes and high glucose environment affected the uptake of oxLDL in the BMDM cells in vitro, although there was no genotype difference in the CD36 level. Pioglitazone enhances CD36 level in myeloid cells and BMDMs in both genotypes and it improved oxLDL uptake in the diabetic BMDM in high glucose environment. Our study provides new insight in the mechanism by which pioglitazone may be a beneficial drug of choice in the treatment of insulin resistance in terms of oxidized lipid clearance, and hence lowering risk in cardiovascular diseases and stroke.

Acknowledgements:

This work was supported by NIH grant R01 NS102886 (JL), VA merit award I01BX003335 (JL), Research Career Scientist award IK6BX004600 (JL). The authors would like to thank Dr. Brant Watson for comments and manuscript editing.

References

Aitman TJ, Cooper LD, Norsworthy PJ, Wahid FN, Gray JK, Curtis BR, . . . Scott J. (2000). Malaria susceptibility and CD36 mutation. Nature, 405(6790), 1015–1016. doi:10.1038/35016636 [PubMed: 10890433]

Akamatsu Y, Nishijima Y, Lee CC, Yang SY, Shi L, An L, . . . Liu J. (2015). Impaired leptomeningeal collateral flow contributes to the poor outcome following experimental stroke in the Type 2 diabetic mice. J Neurosci, 35(9), 3851–3864. doi:10.1523/JNEUROSCI.3838-14.2015 [PubMed: 25740515]

Bisgaard LS, Mogensen CK, Rosendahl A, Cucak H, Nielsen LB, Rasmussen SE, & Pedersen TX (2016). Bone marrow-derived and peritoneal macrophages have different inflammatory response to oxLDL and M1/M2 marker expression - implications for atherosclerosis research. Sci Rep, 6, 35234. doi:10.1038/srep35234 [PubMed: 27734926]

Cho S, Park EM, Febbraio M, Anrather J, Park L, Racchumi G, . . . Iadecola C. (2005). The class B scavenger receptor CD36 mediates free radical production and tissue injury in cerebral ischemia. J Neurosci, 25(10), 2504–2512. doi:10.1523/JNEUROSCI.0035-05.2005 [PubMed: 15758158]

Coburn CT, Knapp FF Jr., Febbraio M, Beets AL, Silverstein RL, & Abumrad NA (2000). Defective uptake and utilization of long chain fatty acids in muscle and adipose tissues of CD36 knockout mice. J Biol Chem, 275(42), 32523–32529. doi:10.1074/jbc.M003826200 [PubMed: 10913136]

Cushing SD, Berliner JA, Valente AJ, Territo MC, Navab M, Parhami F, . . . Fogelman AM (1990). Minimally modified low density lipoprotein induces monocyte chemotactic protein 1 in human endothelial cells and smooth muscle cells. Proc Natl Acad Sci U S A, 87(13), 5134–5138. doi:10.1073/pnas.87.13.5134 [PubMed: 1695010]

Driscoll WS, Vaisar T, Tang J, Wilson CL, & Raines EW (2013). Macrophage ADAM17 deficiency augments CD36-dependent apoptotic cell uptake and the linked anti-inflammatory phenotype. Circ Res, 113(1), 52–61. doi:10.1161/CIRCRESAHA.112.300683 [PubMed: 23584255]

Emerging Risk Factors, C., Sarwar N, Gao P, Seshasai SR, Gobin R, Kaptoge S, . . . Danesh J. (2010). Diabetes mellitus, fasting blood glucose concentration, and risk of vascular disease: a collaborative meta-analysis of 102 prospective studies. Lancet, 375(9733), 2215–2222. doi:10.1016/S0140-6736(10)60484-9 [PubMed: 20609967]

Engstrom G, Stavenow L, Hedblad B, Lind P, Eriksson KF, Janzon L, & Lindgarde F. (2003). Inflammation-sensitive plasma proteins, diabetes, and mortality and incidence of myocardial infarction and stroke: a population-based study. Diabetes, 52(2), 442–447. doi:10.2337/diabetes.52.2.442 [PubMed: 12540619]

Eto M, Sumi H, Fujimura H, Yoshikawa H, & Sakoda S. (2008). Pioglitazone promotes peripheral nerve remyelination after crush injury through CD36 upregulation. J Peripher Nerv Syst, 13(3), 242–248. doi:10.1111/j.1529-8027.2008.00183.x [PubMed: 18844791]

Fang H, Chen J, Lin S, Wang P, Wang Y, Xiong X, & Yang Q. (2014). CD36-mediated hematoma absorption following intracerebral hemorrhage: negative regulation by TLR4 signaling. J Immunol, 192(12), 5984–5992. doi:10.4049/jimmunol.1400054 [PubMed: 24808360]

Febbraio M, Hajjar DP, & Silverstein RL (2001). CD36: a class B scavenger receptor involved in angiogenesis, atherosclerosis, inflammation, and lipid metabolism. J Clin Invest, 108(6), 785–791. doi:10.1172/JCI14006 [PubMed: 11560944]

Febbraio M, Podrez EA, Smith JD, Hajjar DP, Hazen SL, Hoff HF, . . . Silverstein RL (2000). Targeted disruption of the class B scavenger receptor CD36 protects against atherosclerotic lesion development in mice. J Clin Invest, 105(8), 1049–1056. doi:10.1172/JCI9259 [PubMed: 10772649]

Fernandez-Boyanapalli RF, Frasch SC, Thomas SM, Malcolm KC, Nicks M, Harbeck RJ, . . . Bratton DL (2015). Pioglitazone restores phagocyte mitochondrial oxidants and bactericidal capacity in

chronic granulomatous disease. J Allergy Clin Immunol, 135(2), 517–527 e512. doi:10.1016/j.jaci.2014.10.034 [PubMed: 25498313]

Fuentes B, Castillo J, San Jose B, Leira R, Serena J, Vivancos J, . . . Stroke Project of the Cerebrovascular Diseases Study Group, S. S. o. N. (2009). The prognostic value of capillary glucose levels in acute stroke: the GLycemia in Acute Stroke (GLIAS) study. Stroke, 40(2), 562–568. doi:10.1161/STROKEAHA.108.519926 [PubMed: 19095970]

Greenlee-Wacker MC (2016). Clearance of apoptotic neutrophils and resolution of inflammation. Immunol Rev, 273(1), 357–370. doi:10.1111/imr.12453 [PubMed: 27558346]

Griffin E, Re A, Hamel N, Fu C, Bush H, McCaffrey T, & Asch AS (2001). A link between diabetes and atherosclerosis: Glucose regulates expression of CD36 at the level of translation. Nat Med, 7(7), 840–846. doi:10.1038/89969 [PubMed: 11433350]

Hajri T, Ibrahimi A, Coburn CT, Knapp FF Jr., Kurtz T, Pravenec M, & Abumrad NA (2001). Defective fatty acid uptake in the spontaneously hypertensive rat is a primary determinant of altered glucose metabolism, hyperinsulinemia, and myocardial hypertrophy. J Biol Chem, 276(26), 23661–23666. doi:10.1074/jbc.M100942200 [PubMed: 11323420]

Handberg A, Norberg M, Stenlund H, Hallmans G, Attermann J, & Eriksson JW (2010). Soluble CD36 (sCD36) clusters with markers of insulin resistance, and high sCD36 is associated with increased type 2 diabetes risk. J Clin Endocrinol Metab, 95(4), 1939–1946. doi:10.1210/jc.2009-2002 [PubMed: 20139232]

Hirano K, Kuwasako T, Nakagawa-Toyama Y, Janabi M, Yamashita S, & Matsuzawa Y. (2003). Pathophysiology of human genetic CD36 deficiency. Trends Cardiovasc Med, 13(4), 136–141. Retrieved from https://www.ncbi.nlm.nih.gov/pubmed/12732446 [PubMed: 12732446]

Jiang C, Liu Z, Hu R, Bo L, Minshall RD, Malik AB, & Hu G. (2017). Inactivation of Rab11a GTPase in Macrophages Facilitates Phagocytosis of Apoptotic Neutrophils. J Immunol, 198(4), 1660–1672. doi:10.4049/jimmunol.1601495 [PubMed: 28053235]

Kilkenny C, Browne W, Cuthill IC, Emerson M, Altman DG, National Centre for the Replacement, R., & Reduction of Amimals in, R. (2011). Animal research: reporting in vivo experiments--the ARRIVE guidelines. J Cereb Blood Flow Metab, 31(4), 991–993. doi:10.1038/jcbfm.2010.220 [PubMed: 21206507]

Kim EH, Tolhurst AT, Szeto HH, & Cho SH (2015). Targeting CD36-mediated inflammation reduces acute brain injury in transient, but not permanent, ischemic stroke. CNS Neurosci Ther, 21(4), 385–391. doi:10.1111/cns.12326 [PubMed: 25216018]

Liang CP, Han S, Okamoto H, Carnemolla R, Tabas I, Accili D, & Tall AR (2004). Increased CD36 protein as a response to defective insulin signaling in macrophages. J Clin Invest, 113(5), 764–773. doi:10.1172/JCI19528 [PubMed: 14991075]

Liu HY, Cui HB, Chen XM, Chen XY, Wang SH, Du WP, . . . Huang C. (2014). Imbalanced response of ATP-binding cassette transporter A1 and CD36 expression to increased oxidized low-density lipoprotein loading contributes to the development of THP-1 derived foam cells. J Biochem, 155(1), 35–42. doi:10.1093/jb/mvt106 [PubMed: 24394674]

Lusis AJ (2000). Atherosclerosis. Nature, 407(6801), 233–241. doi:10.1038/35025203 [PubMed: 11001066]

Martini SR, & Kent TA (2007). Hyperglycemia in acute ischemic stroke: a vascular perspective. J Cereb Blood Flow Metab, 27(3), 435–451. doi:10.1038/sj.jcbfm.9600355 [PubMed: 16804552]

Megherbi SE, Milan C, Minier D, Couvreur G, Osseby GV, Tilling K, . . . European, B. S. o. S. C. G. (2003). Association between diabetes and stroke subtype on survival and functional outcome 3 months after stroke: data from the European BIOMED Stroke Project. Stroke, 34(3), 688–694. doi:10.1161/01.STR.0000057975.15221.40 [PubMed: 12624292]

Miyaoka K, Kuwasako T, Hirano K, Nozaki S, Yamashita S, & Matsuzawa Y. (2001). CD36 deficiency associated with insulin resistance. Lancet, 357(9257), 686–687. doi:10.1016/s0140-6736(00)04138-6 [PubMed: 11247555]

Nagy L, Tontonoz P, Alvarez JG, Chen H, & Evans RM (1998). Oxidized LDL regulates macrophage gene expression through ligand activation of PPARgamma. Cell, 93(2), 229–240. doi:10.1016/s0092-8674(00)81574-3 [PubMed: 9568715]

Pain A, Urban BC, Kai O, Casals-Pascual C, Shafi J, Marsh K, & Roberts DJ (2001). A non-sense mutation in Cd36 gene is associated with protection from severe malaria. Lancet, 357(9267), 1502–1503. doi:10.1016/S0140-6736(00)04662-6 [PubMed: 11377606]

Parsons MW, Barber PA, Desmond PM, Baird TA, Darby DG, Byrnes G, . . . Davis SM (2002). Acute hyperglycemia adversely affects stroke outcome: a magnetic resonance imaging and spectroscopy study. Ann Neurol, 52(1), 20–28. doi:10.1002/ana.10241 [PubMed: 12112043]

Percie du Sert N, Hurst V, Ahluwalia A, Alam S, Avey MT, Baker M, . . . Würbel H. (2019). The ARRIVE guidelines 2019: updated guidelines for reporting animal research. bioRxiv, 703181. doi:10.1101/703181

Puente Navazo MD, Daviet L, Ninio E, & McGregor JL (1996). Identification on human CD36 of a domain (155–183) implicated in binding oxidized low-density lipoproteins (Ox-LDL). Arterioscler Thromb Vasc Biol, 16(8), 1033–1039. doi:10.1161/01.atv.16.8.1033 [PubMed: 8696943]

Quinn MT, Parthasarathy S, Fong LG, & Steinberg D. (1987). Oxidatively modified low density lipoproteins: a potential role in recruitment and retention of monocyte/macrophages during atherogenesis. Proc Natl Acad Sci U S A, 84(9), 2995–2998. doi:10.1073/pnas.84.9.2995 [PubMed: 3472245]

Rathinam VA, Vanaja SK, & Fitzgerald KA (2012). Regulation of inflammasome signaling. Nat Immunol, 13(4), 333–342. doi:10.1038/ni.2237 [PubMed: 22430786]

Sampson MJ, Davies IR, Braschi S, Ivory K, & Hughes DA (2003). Increased expression of a scavenger receptor (CD36) in monocytes from subjects with Type 2 diabetes. Atherosclerosis, 167(1), 129–134. doi:10.1016/s0021-9150(02)00421-5 [PubMed: 12618277]

Sheedy FJ, Grebe A, Rayner KJ, Kalantari P, Ramkhelawon B, Carpenter SB, . . . Moore KJ (2013). CD36 coordinates NLRP3 inflammasome activation by facilitating intracellular nucleation of soluble ligands into particulate ligands in sterile inflammation. Nat Immunol, 14(8), 812–820. doi:10.1038/ni.2639 [PubMed: 23812099]

Tabas I, Williams KJ, & Boren J. (2007). Subendothelial lipoprotein retention as the initiating process in atherosclerosis: update and therapeutic implications. Circulation, 116(16), 1832–1844. doi:10.1161/CIRCULATIONAHA.106.676890 [PubMed: 17938300]

Tontonoz P, Nagy L, Alvarez JG, Thomazy VA, & Evans RM (1998). PPARgamma promotes monocyte/macrophage differentiation and uptake of oxidized LDL. Cell, 93(2), 241–252. doi:10.1016/s0092-8674(00)81575-5 [PubMed: 9568716]

Wang C, Yu X, Cao Q, Wang Y, Zheng G, Tan TK, . . . Harris D. (2013). Characterization of murine macrophages from bone marrow, spleen and peritoneum. BMC Immunol, 14, 6. doi:10.1186/1471-2172-14-6 [PubMed: 23384230]

Williams KJ, & Tabas I. (1995). The response-to-retention hypothesis of early atherogenesis. Arterioscler Thromb Vasc Biol, 15(5), 551–561. doi:10.1161/01.atv.15.5.551 [PubMed: 7749869]

Woo MS, Wang X, Faustino JV, Derugin N, Wendland MF, Zhou P, . . . Vexler ZS (2012). Genetic deletion of CD36 enhances injury after acute neonatal stroke. Ann Neurol, 72(6), 961–970. doi:10.1002/ana.23727 [PubMed: 23280844]

Woo MS, Yang J, Beltran C, & Cho S. (2016). Cell Surface CD36 Protein in Monocyte/Macrophage Contributes to Phagocytosis during the Resolution Phase of Ischemic Stroke in Mice. J Biol Chem, 291(45), 23654–23661. doi:10.1074/jbc.M116.750018 [PubMed: 27646002]

Yaghi S, Furie KL, Viscoli CM, Kamel H, Gorman M, Dearborn J, . . . Investigators, I. T. (2018). Pioglitazone Prevents Stroke in Patients With a Recent Transient Ischemic Attack or Ischemic Stroke: A Planned Secondary Analysis of the IRIS Trial (Insulin Resistance Intervention After Stroke). Circulation, 137(5), 455–463. doi:10.1161/CIRCULATIONAHA.117.030458 [PubMed: 29084736]

Yamashita S, Hirano K, Kuwasako T, Janabi M, Toyama Y, Ishigami M, & Sakai N. (2007). Physiological and pathological roles of a multi-ligand receptor CD36 in atherogenesis; insights from CD36-deficient patients. Mol Cell Biochem, 299(1–2), 19–22. doi:10.1007/s11010-005-9031-4 [PubMed: 16670819]

Yang J, Park KW, & Cho S. (2018). Inhibition of the CD36 receptor reduces visceral fat accumulation and improves insulin resistance in obese mice carrying the BDNF-Val66Met variant. J Biol Chem, 293(34), 13338–13348. doi:10.1074/jbc.RA118.002405 [PubMed: 29914985]

Yuasa-Kawase M, Masuda D, Yamashita T, Kawase R, Nakaoka H, Inagaki M, . . . Yamashita S. (2012). Patients with CD36 deficiency are associated with enhanced atherosclerotic cardiovascular diseases. J Atheroscler Thromb, 19(3), 263–275. doi:10.5551/jat.10603 [PubMed: 22075538]

Highlights

- CD36 levels markedly reduced in myeloid cells of the adult but not of juvenile T2DM mice
- Soluble CD36 levels increased in the adult T2DM mice
- T2DM or high glucose impairs uptake of oxLDL in BMDM cells
- Pioglitazone enhances CD36 levels in diabetic cells and oxLDL uptake

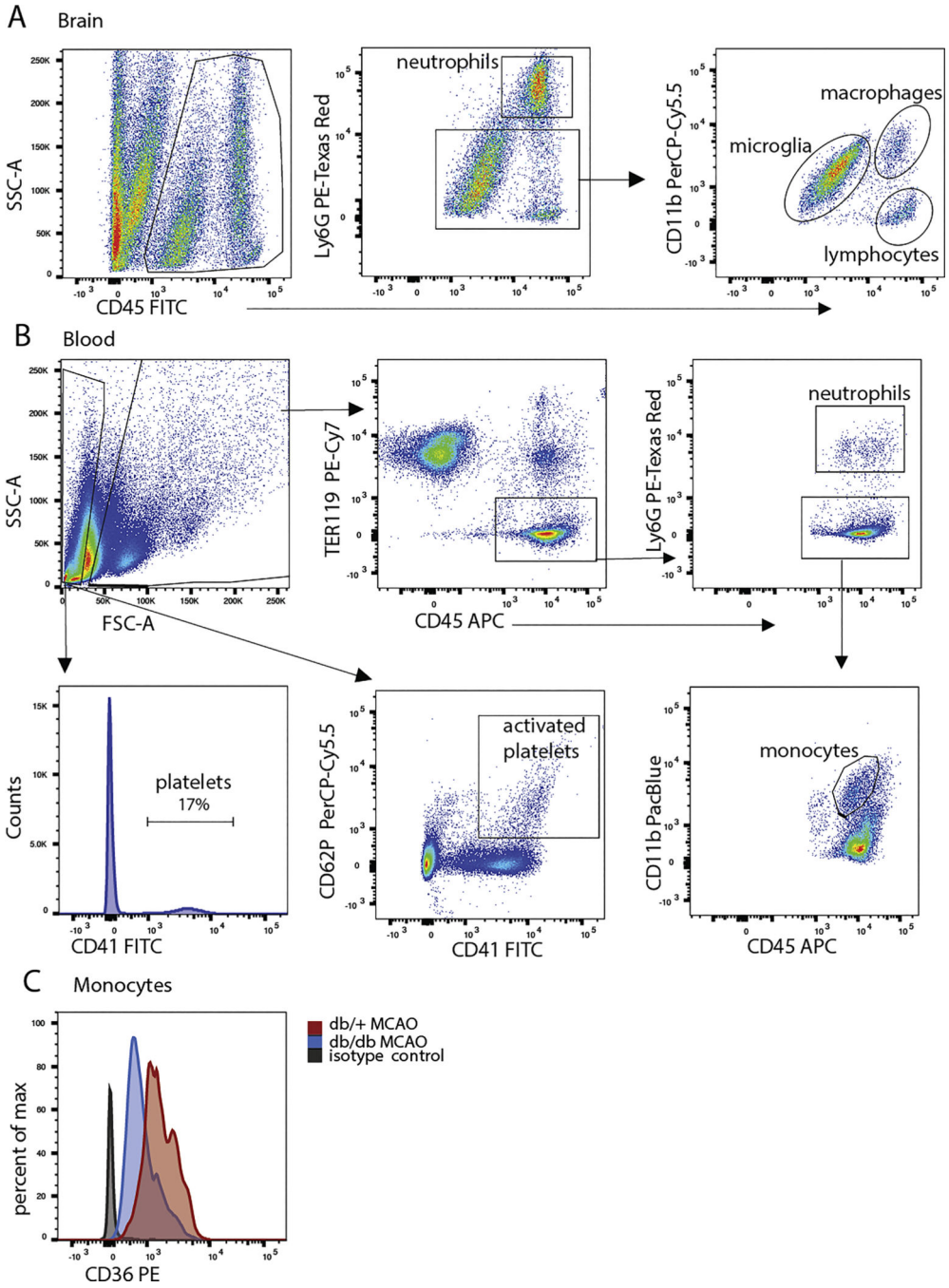

Figure 1. Flow cytometry gating schemes for the comparison of CD36 expression among various myeloid populations in the brain or blood.

Representative sequential gating of cells from the brain tissues (A) and blood (B) is shown to isolate myeloid cells. The markers used for cell type identification were: neutrophils ($CD45^{hi}/Ly6G^{hi)}$, monocytes/macrophages ($CD45^{hi}/Ly6G^{low}/CD11b^{hi)}$, lymphocytes ($CD45^{hi}/Ly6G^{low}/CD11b^{low)}$, microglia ($CD45^{int}/Ly6G^{low}/CD11b^{hi)}$. Platelets were identified by CD41 expression. Appropriate isotype control was used to establish the threshold of CD36 positive staining. C, representative fluorescent intensity for IgG2a kappa-PE and CD36-PE for each genotype is shown in the histogram.

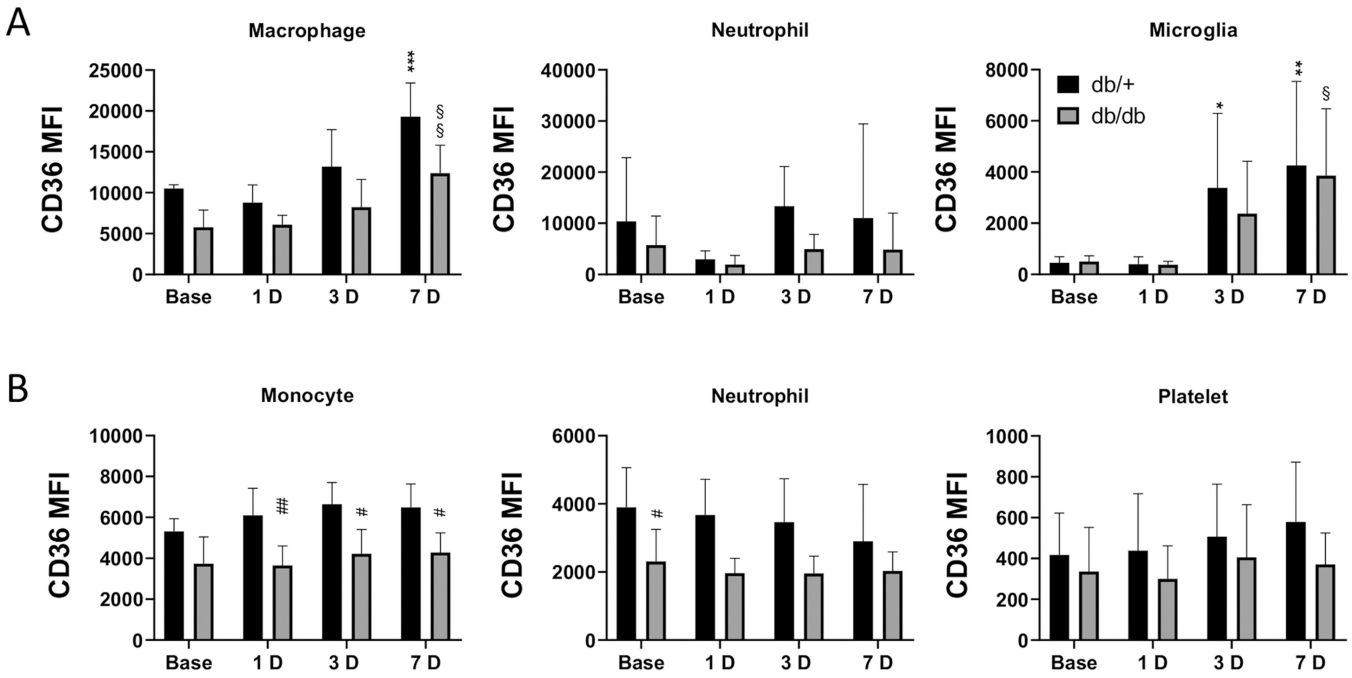

Figure 2. CD36 expression on the cell surface of neutrophils and monocytes is significantly reduced in the diabetic mice.

The temporal changes of CD36 mean fluorescence intensity (MFI) of infiltrating cells in brain (**A**) and in peripheral blood (**B**) of the adult db/+ and db/db mice were shown from baseline, 1, 3 and 7 days after MCAO. CD36 was significantly increased 7 days after stroke in brain macrophages in both db/+ and db/db mice. Microglia CD36 level was increased at 3 and 7 days after stroke in db/+ mice, compared to increase at 7 days after stroke in db/db. Monocytes and neutrophils in db/db blood expressed a significantly less level of CD36 than those in db/+ mice after stroke and at baseline, respectively. Time point vs. baseline: *, **, ***: P<0.05, 0.01, 0.005 (db/+); §, §§: P<0.05, 0.01 (db/db). Genotype difference: #, ##, ###: P<0.05, 0.01, 0.005. N=5/genotype.

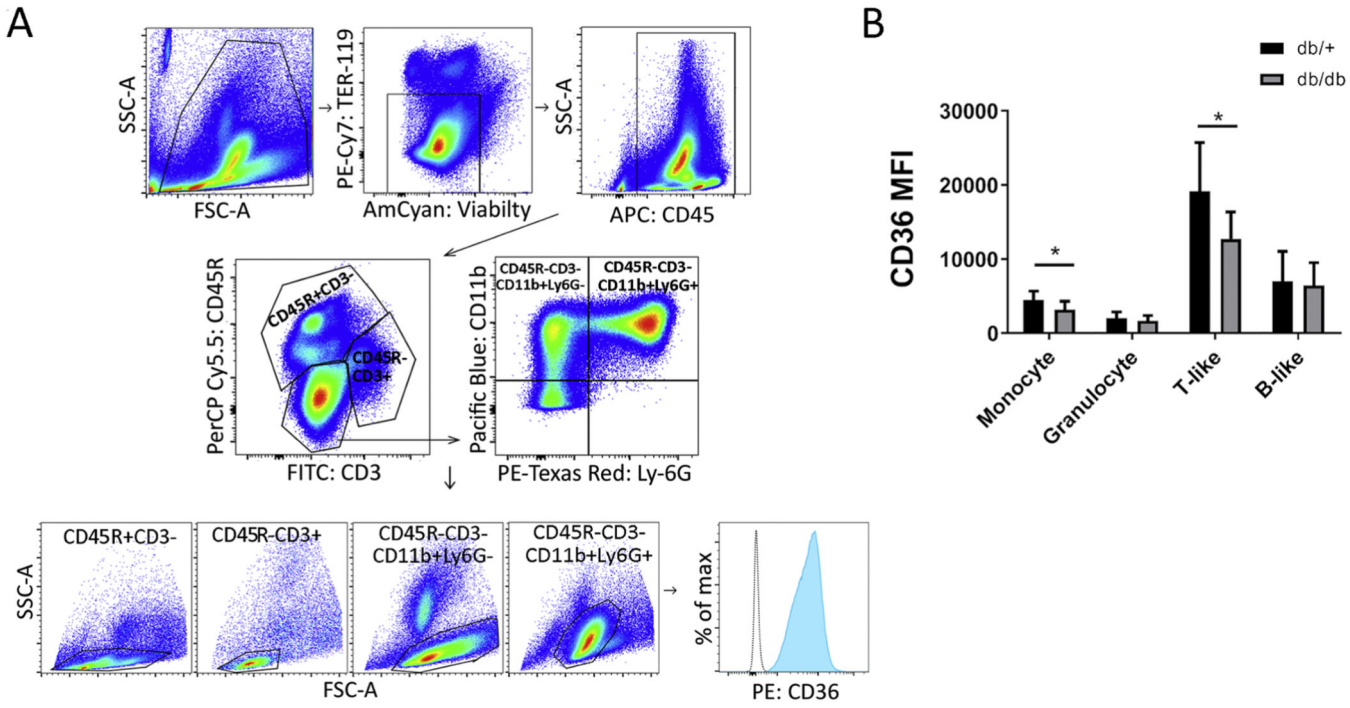

Figure 3. CD36 expression on cell surface of bone marrow monocytes and T cells is significantly reduced in the diabetic mice.

A, CD45+ cells were gated from viable cells and further divided into B-like ($CD3^{low}CD45R^{hi}$), T-like ($CD3^{hi}CD45R^{low}$) and non-T/non-B cells ($CD3^{low}CD45R^{low}$). Monocytes ($CD11b^{+}Ly6G^{-}$) from non-T/non-B cells were gated from granulocytes ($CD11b^{+}Ly6G^{+}$). **B**, Mean fluorescence intensity (MFI) for CD36 staining was determined by subtracting the signal (blue shade) from that of isotype control (IgG2a) (left curve in histogram). CD36 MFI was significantly reduced in monocytes and T-like cells isolated from BM of db/db mice compared to db/+ mice. *P<0.05. N=6/genotype.

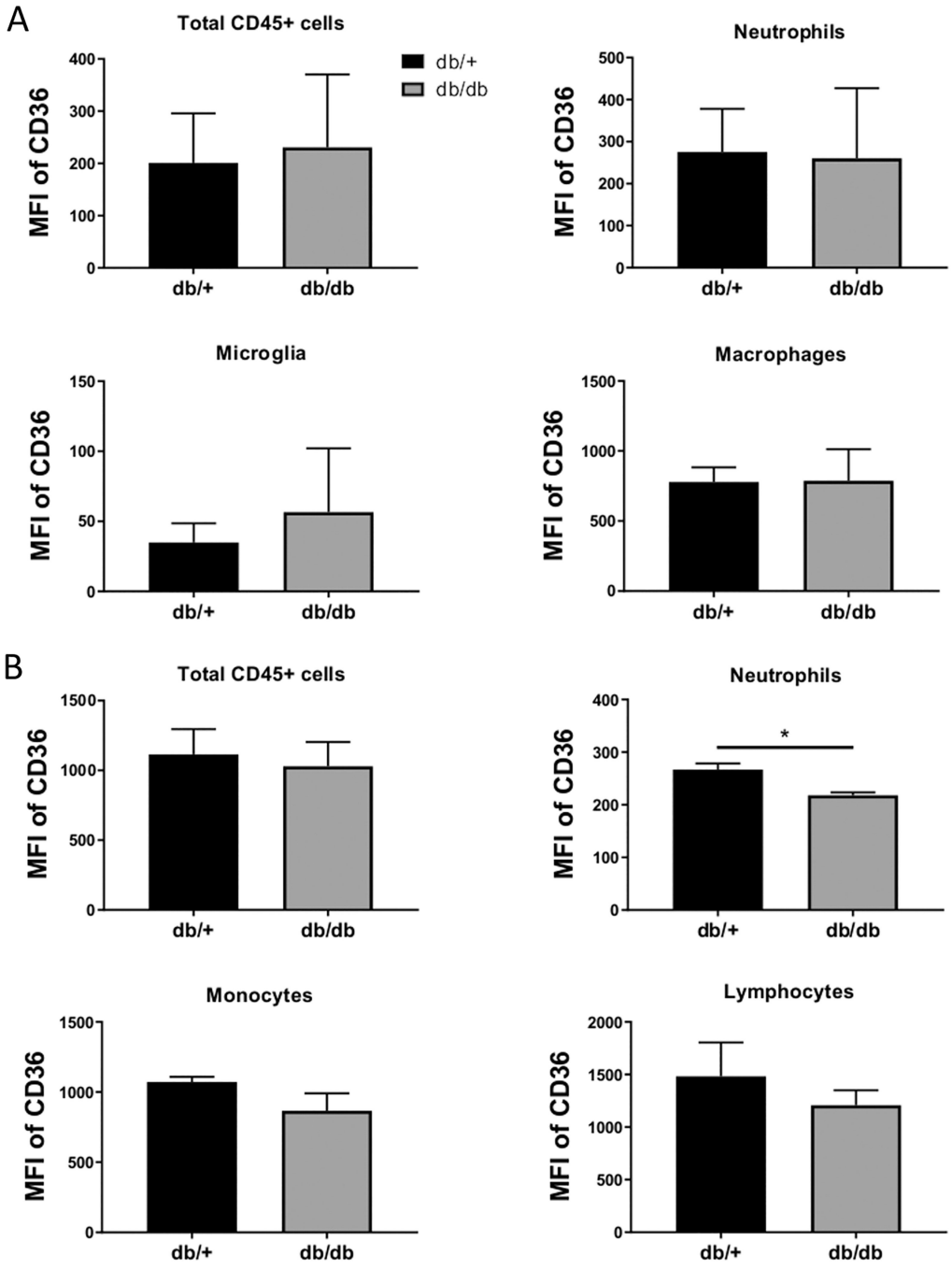

Figure 4. CD36 expression on immune cells in the brain and blood of 3-week old mice.

MFI of CD36 determined by FACS was similar in many myeloid cell types isolated from the brain (A) and blood (B) between juvenile db/+ and db/db mice except for blood neutrophils, which showed a mild reduction in the db/db mice.

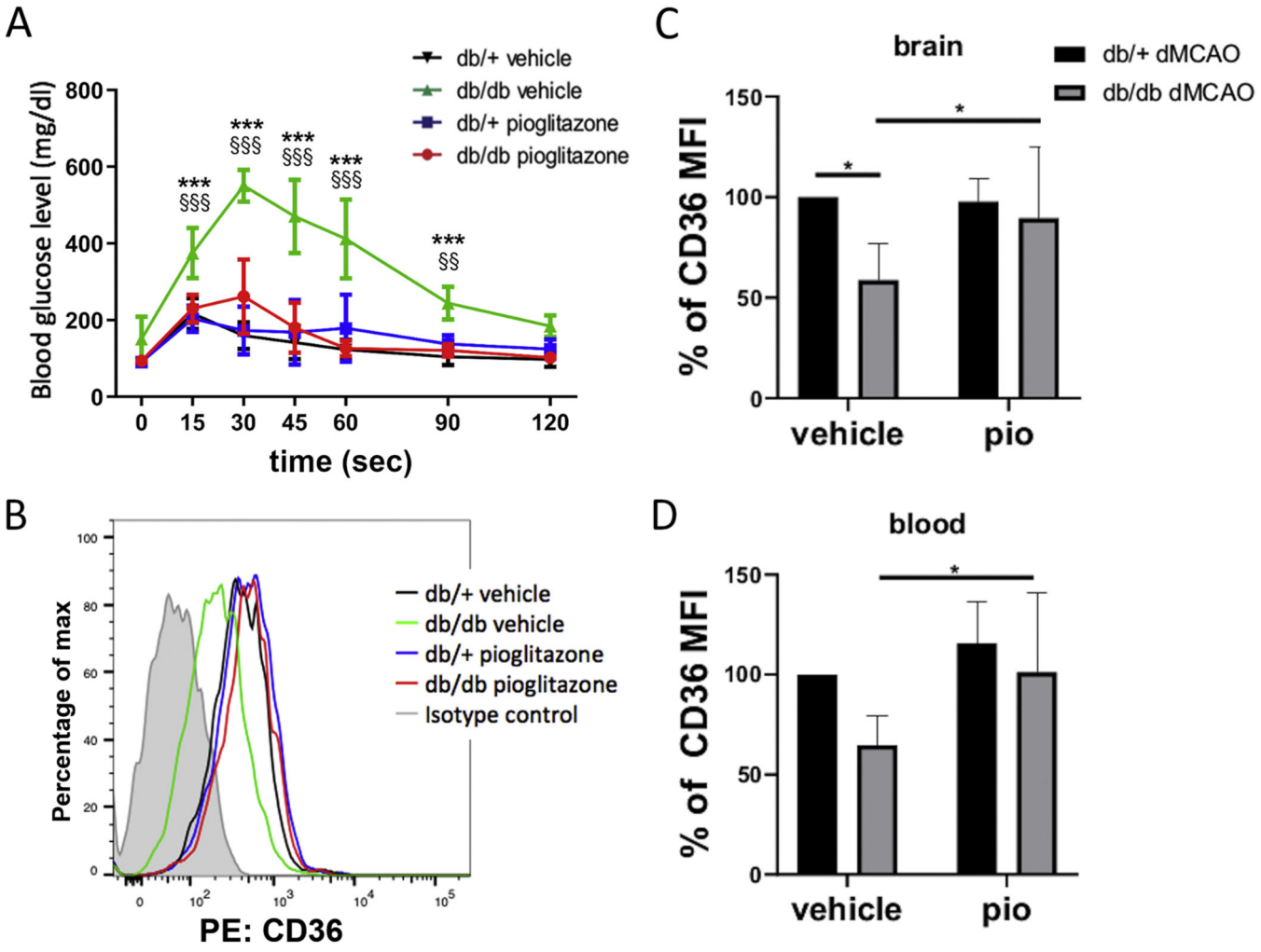

Figure 5. The effect of pioglitazone oral treatment on insulin sensitivity and the level of CD36.

A, The results of the oral glucose tolerance test. Blood glucose level in vehicle-treated db/db mice was significantly higher than that in db/+ 15 to 90 minutes after glucose administration (§§, §§§: P<0.01, 0.005). Following pioglitazone treatment for four weeks, blood glucose level in db/db mice was significantly less than that in vehicle-treated db/db (***: P<0.001). N=3/treatment group/db+; N=5/treatment group/db/db. **B,** A representative FACS plot showing CD36 surface expression in each mouse strain after vehicle or pioglitazone treatment in $CD45^{hi}/CD11b^{hi}$ myeloid cells isolated from the brains. **C, D**, Relative % of CD36 mean fluorescence intensity (MFI) in groups after setting the MFI of db+ cells in the vehicle group as 100%. Pioglitazone significantly increased the MFI in the db/db myeloid cells from the brain and blood. N= 4/db/+; N=5/db/db.

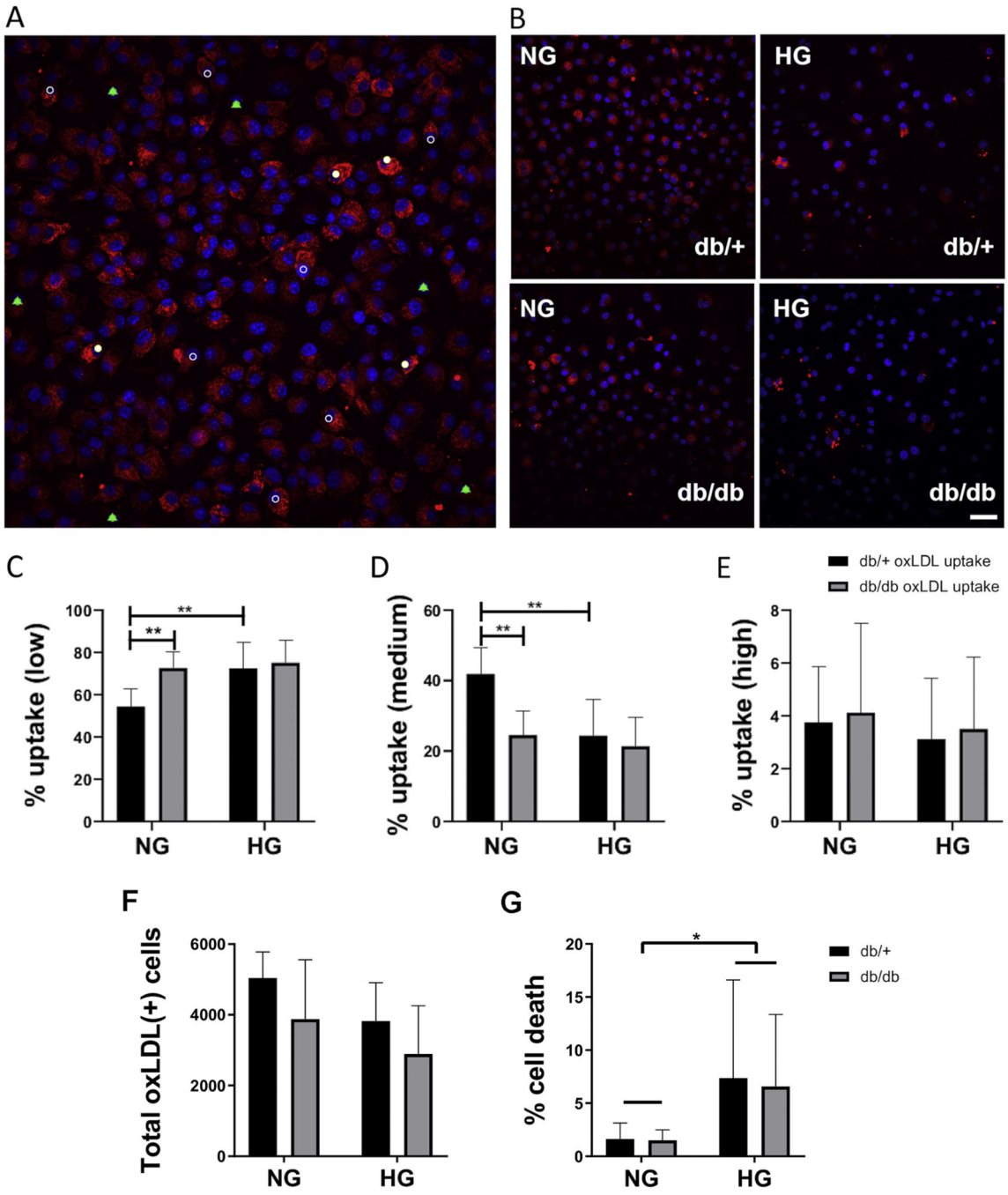

Figure 6. T2DM or hyperglycemia interferes with oxLDL uptake.

A, the amount of DiI-oxLDL uptake in BMDM cells was divided into low or no uptake (green bell), medium uptake (white circle) and high uptake (solid white) category, depending on the fluorochrome intensity of the DiI determined by Fiji and presented as percentage of positive cells with respect to total cell number in that category in the bar graphs below. **B**, Representative images of DiI labeled oxLDL uptake in from db/+ or db/db BMDM cells cultured in normal glucose (NG)- or high glucose (HG)-containing medium. **C-E,** Two-way ANOVA with Tukey's multiple comparisons test was used to analyze the data. In the

normoglycemic (NG) condition fewer db/+ BMDM cells displayed low or no uptake of DiI ox-LDL compared to that of db/db cells ($P< 0.01$). There are also more db/+ BMDM cells with low/no uptake in the hyperglycemic (HG) culture compared to NG culture condition ($P<0.01$). A significant reduction ($P<0.01$) of cells number with medium level of uptake was found in the db/db BMDM compared to that of db+ cells when cultured in the NG medium. Moreover, DiI ox-LDL uptake was significantly reduced in db/+ BMDM in HG compared to NG medium ($P<0.01$). No significant difference was detected between conditions or genotypes with high uptake, likely representing non-specific binding that was seen in very few cells. **F**, There was a trending global effect of high glucose environment on the total number of cells taken up oxLDL (glucose effect: $P= 0.06$). **G**, Hyperglycemia also increased cell death (glucose effect: $P< 0.05$). *$P<0.05$, **$P<0.01$. N=8/group. Scale bar: 10μm.

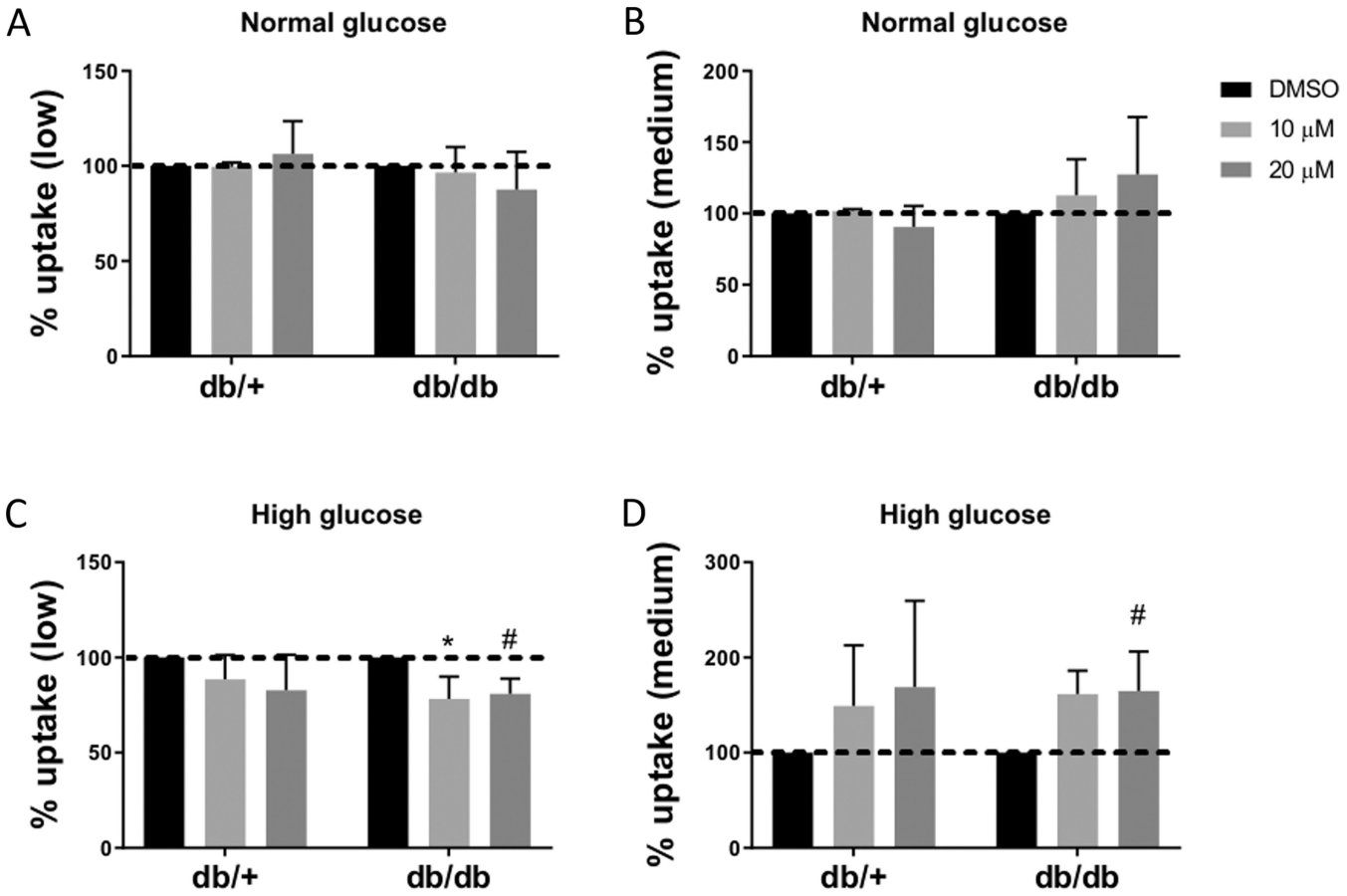

Figure 7. The effect of pioglitazone on the uptake of DiI-oxLDL in vitro.

BMDM from db/+ or db/db mice were cultured in the normoglycemic (A, B) or hyperglycemic medium (C, D) in the presence of 10 μM or 20 μM of pioglitazone or vehicle control (0.1% DMSO). The uptake level is shown in the low and medium categories. Pioglitazone reduced the percentage of cells with a low/no uptake while promoting a borderline increase in oxLDL uptake in the medium uptake category for db/db BMDM cells cultured in the hyperglycemic medium. *P<0.05, #P=0.065. N=3/group.

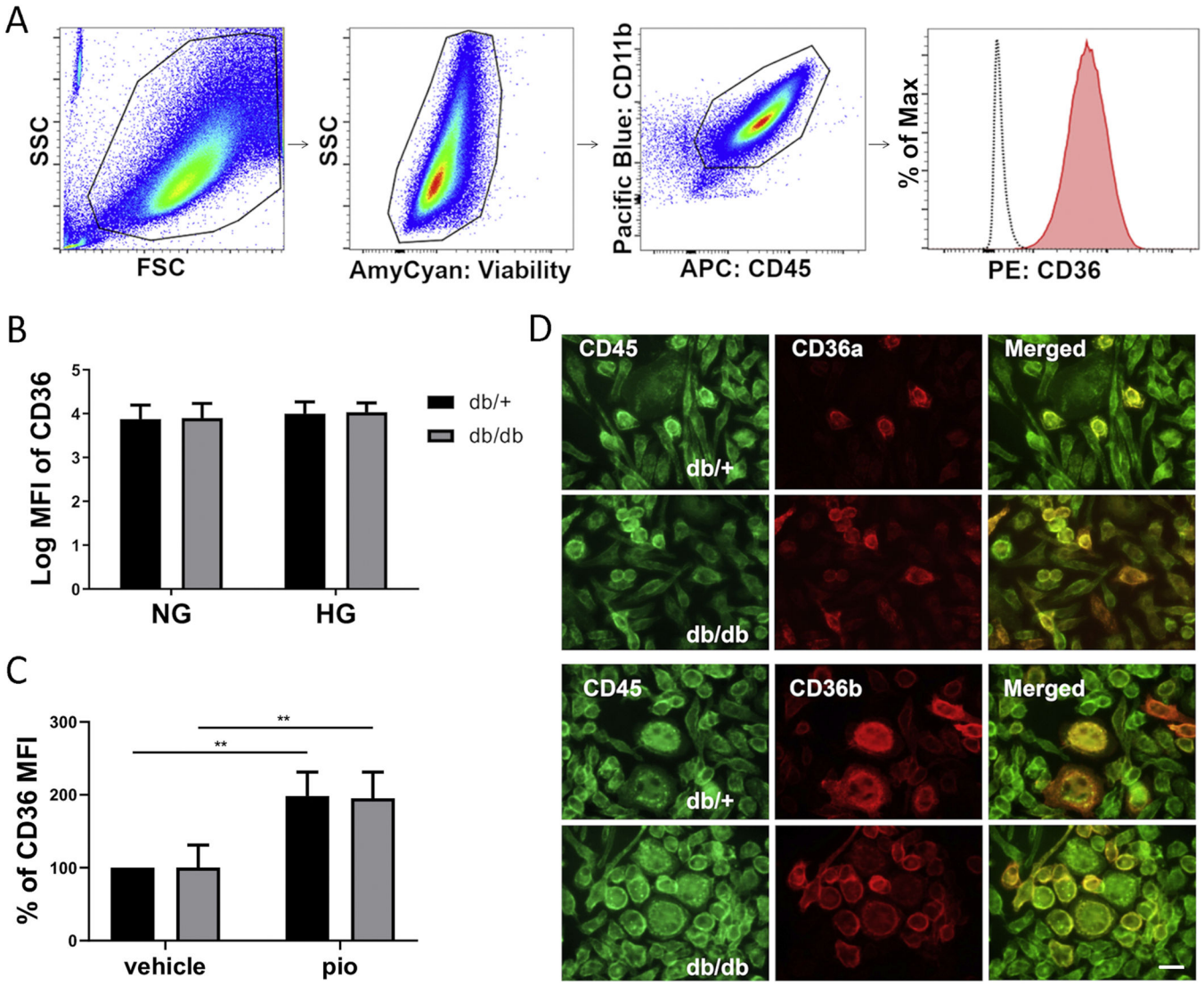

Figure 8. High level of CD36 expression was detected on both db/+ and db/db BMDM cells.

A, A representative FACS scheme for the quantification of CD36 in db/+ BMDMs in normal glucose medium, **B**, the column graph showed that there was no significant difference in CD36 expression between genotypes or between medium environment with normal- (NG) and high glucose (HG) concentrations. NG: N=7/genotype; HG: N=11/genotype. **C**, Pioglitazone enhanced CD36 MFI in BMDM cells from db/+ and db/db mice in a similar manner (N=4/group). **: P<0.01. **D**, Double immunofluorescence staining of BMDM cells by CD45 (green) and CD36 (red) and merged images. Following differentiation of bone marrow leukocytes in MCSF containing medium for one week, almost all the cells expressed CD45 marker from both strains. CD36a and CD36b correspond to staining using two different CD36 antibodies, i.e. clone 72–1 (eBioscience) and CRF D-2712 (BD Pharmingen), respectively. There was no apparent difference in CD36 staining pattern between genotypes as detected by either antibody. Scale bar: 10μm.